

- Adrian, T, De Wever O. Frondoside A suppressive effects on lung cancer survival, tumor growth, angiogenesis, invasion, and metastasis. **PLoS ONE**8:e53087, 2013. doi: 10.1371/journal.pone.0053087.
- 5 Matsuura S, Kahyo T, Shinmura K, Iwaizumi M, Yamada H, Funai K, Kobayashi J, Tanahashi M, Niwa H, Ogawa H, Takahashi T, Inui N, Suda T, Chida K, Watanabe Y, Sugimura H. SGOL1 variant B induces abnormal mitosis and resistance to taxane in non-small cell lung cancers. **Sci Rep.** 3: 2013. doi: 10.1038/srep03012.
  - 6 Arafat K, Iratni R, Takahashi T, Parekh K, Al Dhaheri Y, Adrian TE, Attoub S. Inhibitory effects of salinomycin on cell survival, colony growth, migration, and invasion of human non-small cell lung cancer A549 and LNM35: Involvement of NAG-1. **PLoS ONE**, 8:e66931, 2013. DOI: 10.1371/journal.pone.0066931
  - 7 Roth FC, Mulder JE, Brien JF, Takahashi T, Massey TE. Cytotoxic interaction between amiodarone and desethylamiodarone in human peripheral lung epithelial cells. **Chem Biol Interact.** 204:135-139, 2013.
  - 8 Yamashita Y, Akatsuka S, Shinjo K, Yatabe Y, Kobayashi H, Seko H, Kajiyama H, Kikkawa F, Takahashi T, Toyokuni S. Met is the most frequently amplified gene in endometriosis-associated ovarian clear cell adenocarcinoma and correlates with worsened prognosis. **PLoS ONE**. 8:e57724, 2013. doi: 10.1371/journal.pone.0057724.
  - 9 Ishiguro F, Murakami H, Mizuno T, Fujii M, Kondo Y, Usami N, Taniguchi T, Yokoi K, Osada H, Sekido Y. Membranous expression of activated leukocyte cell adhesion molecule contributes to poor prognosis and malignant phenotypes of non-small-cell lung cancer. **J Surg Res.** 179: 24-32, 2013.
  - 10 Shinjo K, Yamashita Y, Yamamoto E, Akatsuka S, Uno N, Kamiya A, Niimi K, Sakaguchi Y, Nagasaka T, Takahashi T, Shibata K, Kajiyama H, Kikkawa F, Toyokuni S. Expression of chromobox homolog 7 (CBX7) is associated with poor prognosis in ovarian clear cell adenocarcinoma via TRAIL-induced apoptotic pathway regulation. **Int J Cancer.** (in press)
  - 11 Chew SH, Okazaki Y, Nagai H, Misawa N, Akatsuka S, Yamashita K, Jiang L, Yamashita Y, Noguchi M, Hosoda K, Sekido Y, Takahashi T, Toyokuni S. Cancer-promoting role of adipocytes in asbestos-induced mesothelial carcinogenesis through dysregulated adipocytokine production. **Carcinogenesis** 35:164-172, 2014. DOI: 10.1093/carcin/bgt267
  - 12 Fukatsu A, Ishiguro F, Tanaka I, Kudo T, Nakagawa K, Shinjo K, Kondo Y, Fujii M, Hasegawa Y, Tomizawa K, Mitsudomi T, Osada H, Hata Y, Sekido Y. RASSF3 downregulation increases malignant phenotypes of non-small cell lung cancer. **Lung Cancer.** 83: 23-9, 2014.
  - 13 Okamoto Y, Shinjo K, Shimizu Y, Sano T, Yamao K, Gao W, Fujii M, Osada H, Sekido Y, Murakami S, Tanaka Y, Joh T, Sato S, Takahashi S, Wakita T, Zhu J, Issa JP, Kondo Y. Hepatitis virus infection affects DNA methylation in mice with humanized livers. **Gastroenterol.** 146: 562-72, 2014.
  - 14 Tanaka I, Osada H, Fujii M, Fukatsu A, Hida T, Horio Y, Kondo Y, Sato A, Hasegawa Y, Tsujimura T, Sekido Y. LIM-domain protein AJUBA suppresses malignant mesothelioma cell proliferation via Hippo signaling cascade. **Oncogene** (in press).
  - 15 Fernandez-Cuesta L, Plenker D, Osada H, Sun R, Menon R, Leenders F, Ortiz-Cuaran S, Peifer M, Bos M, DaBler J, Malchers F,

Schottle J, Vogel W, Dahmen I, Koker M, Ullrich RT, Wright GM, Russell PA, Wainer Z, Solomon B, Brambilla E, Nagy-Mignotte H, Moro-Sibilot D, Brambilla CG, Lantuejoul S, Altmuller J, Becker C, Nurnberg P, Heuckmann JM, Stoelben E, Petersen I, Clement JH, Sanger J, Muscarella LA, la Torre A, Fazio VM, Lahortiga I, Perera T, Ogata S, Parade M, Brehmer D, Vingron M, Heukamp LC, Buettner R, Zander T, Wolf J, Perner S, Ansen S, Haas SA, Yatabe Y, Thomas RK. CD74-*NRG1* fusions in lung adenocarcinoma. **Cancer Discov.** 4: 415-22, 2014

a potential target for lung cancer diagnostics and therapeutics. 第36回日本分子生物学会年会（ポスター）、神戸、2013年12月3日 - 6日.

#### F. 知的財産権の出願・登録状況

1. 特許出願
2. 実用新案登録
3. その他  
いずれも、特記すべき事項無し

#### 1 2. 学会発表

- 2 Yanagisawa K, Takahashi T: Proteomic identification of potential biomarkers of human lung malignancies. 第72回日本癌学会学術総会（シンポジウム）、横浜、2013年10月3日-5日.
- 3 Suzuki M, Kato S, Komizu Y, Ueoka R, Arima C, Yanagisawa K, Tamiya-Koizumi K, Murate T, Kyogashima M, Takahashi T: Targeting ceramide homeostasis and metastasis-prone phenotypes in human lung cancer cells. 第72回日本癌学会学術総会（ポスター）、横浜、2013年10月3日-5日.
- 4 Osada H, Yagi K, Yanagisawa K, Akatsuka J, Tatematsu Y, Kato S, Yatabe Y, Ono K, Sekido Y, Takahashi T: Functional analysis of CLCP1 as potential target for lung cancer diagnostics and therapeutics. 第72回日本癌学会学術総会（口演）、横浜、2013年10月3日-5日.
- 5 Osada H, Yagi K, Yanagisawa K, Akatsuka J, Tatematsu Y, Kato S, Yatabe Y, Ono K, Sekido Y, Takahashi T: Analysis of CLCP1,

### III. 研究成果の刊行に関する一覧表

研究成果の刊行に関する一覧表

発表者氏名	論文タイトル名	発表誌名	巻号	ページ	出版年
Tanaka I, <u>Osada H</u> , Fujii M, Fukatsu A, Hida T, Horio Y, Kondo Y, Sato A, Hasegawa Y, Tsujimura T, Sekido Y.	LIM-domain protein AJUBA suppresses malignant mesothelioma cell proliferation via Hippo signaling cascade.	Oncogene			in press
Shinjo K, Yamashita Y, Yamamoto E, Akatsuka S, Uno N, Kamiya A, Niimi K, Sakaguchi Y, Nagasaka T, <u>Takahashi T</u> , Shibata K, Kajiyama H, Kikkawa F, Toyokuni S.	Expression of chromobox homolog 7 (CBX7) is associated with poor prognosis in ovarian clear cell adenocarcinoma via TRAIL-induced apoptotic pathway regulation.	Int J Cancer	135	308-318	2014
Kawahara T, Hotta N, Ozawa Y, Kato S, Kano K, Yokoyama Y, Nagino M, <u>Takahashi T</u> , <u>Yanagisawa K</u> .	Quantitative proteomic profiling identifies DPYSL3 as pancreatic ductal adenocarcinoma-associated molecule that regulates cell adhesion and migration by stabilization of focal adhesion complex.	PloS ONE	8(12)	e79654, 2013. doi: 10.1371/journal.pone.0079654	2013
Yamaguchi T, Hosono Y, <u>Yanagisawa K</u> , <u>Takahashi T</u> .	NKX2-1/TTF-1: an enigmatic oncogene that functions as a double-edged sword for cancer cell survival and progression.	Cancer Cell	23	718-723	2013
Attoub S, Sperandio O, Raza H, Arafat K, Al-Salam S, Al Sultan MA, Al Safi M, <u>Takahashi T</u> , Adem A.	Thymoquinone as an anticancer agent: evidence from inhibition of cancer cells viability and invasion in vitro and tumor growth in vivo.	Fundam Clin Pharmacol	27	557-569	2013
Attoub S, Arafat K, Gelaude A, Sultan MAA, Bracke M, Collin, P, <u>Takahashi T</u> , Adrian, T, De Wever O.	Fronodoside A suppressive effects on lung cancer survival, tumor growth, angiogenesis, invasion, and metastasis.	PLoS ONE	8	e53087, 2013. doi: 10.1371/journal.pone.0053087	2013
Matsuura S, Kahyo T, Shinmura K, Iwaizumi M, Yamada H, Funai K, Kobayashi J, Tanahashi M, Niwa H, Ogawa H, <u>Takahashi T</u> , Inui N, Suda T, Chida K, Watanabe Y, Sugimura H.	SGOL1 variant B induces abnormal mitosis and resistance to taxane in non-small cell lung cancers.	Sci Rep	3	2013. doi: 10.1038/srep03012.	2013
Arafat K, Iratni R, <u>Takahashi T</u> , Parekh K, Al Dhaheri Y, Adrian TE, Attoub S.	Inhibitory effects of salinomycin on cell survival, colony growth, migration, and invasion of human non-small cell lung cancer A549 and LNM35: Involvement of NAG-1.	PLoS ONE	8	2013. DOI: 10.1371/journal.pone.0066931	2013

Roth FC, Mulder JE, Brien JF, <u>Takahashi T</u> , Massey TE.	Cytotoxic interaction between amiodarone and desethylamiodarone in human peripheral lung epithelial cells.	Chem Biol Interact	204	135-139	2013
Yamashita Y, Akatsuka S, Shinjo K, Yatabe Y, Kobayashi H, Seko H, Kajiyama H, Kikkawa F, <u>Takahashi T</u> , Toyokuni S.	Met is the most frequently amplified gene in endometriosis-associated ovarian clear cell adenocarcinoma and correlates with worsened prognosis.	PLoS ONE	8	e57724, 2013. doi: 10.1371/journal.pone.0057724	2013
Ishiguro F, Murakami H, Mizuno T, Fujii M, Kondo Y, Usami N, Taniguchi T, Yokoi K, <u>Osada H</u> , Sekido Y.	Membranous expression of activated leukocyte cell adhesion molecule contributes to poor prognosis and malignant phenotypes of non-small-cell lung cancer.	J Surg Res	179	24-32	2013
Chew SH, Okazaki Y, Nagai H, Misawa N, Akatsuka S, Yamashita K, Jiang L, Yamashita Y, Noguchi M, Hosoda K, Sekido Y, <u>Takahashi T</u> , Toyokuni S.	Cancer-promoting role of adipocytes in asbestos-induced mesothelial carcinogenesis through dysregulated adipocytokine production.	Carcinogenesis	35	164-172	2014
Fukatsu A, Ishiguro F, Tanaka I, Kudo T, Nakagawa K, Shinjo K, Kondo Y, Fujii M, Hasegawa Y, Tomizawa K, Mitsudomi T, <u>Osada H</u> , Hata Y, Sekido Y.	RASSF3 downregulation increases malignant phenotypes of non-small cell lung cancer.	Lung Cancer.	83	23-29	2014
Okamoto Y, Shinjo K, Shimizu Y, Sano T, Yamao K, Gao W, Fujii M, <u>Osada H</u> , Sekido Y, Murakami S, Tanaka Y, Joh T, Sato S, Takahashi S, Wakita T, Zhu J, Issa JP, Kondo Y.	Hepatitis virus infection affects DNA methylation in mice with humanized livers.	Gastroenterol	146	562-572	2014
Fernandez-Cuesta L, Plenker D, <u>Osada H</u> , Sun R, Menon R, Leenders F, Ortiz-Cuaran S, Peifer M, Bos M, DaBler J, Malchers F, Schottle J, Vogel W, Dahmen I, Koker M, Ullrich RT, Wright GM, Russell PA, Wainer Z, Solomon B, Brambilla E, Nagy-Mignotte H, Moro-Sibilot D, Brambilla CG, Lantuejoul S, Altmuller J, Becker C, Nurnberg P, Heuckmann JM, Stoelben E, Petersen I, Clement JH, Sanger J, Muscarella LA, la Torre A, Fazio VM, Lahortiga I, Perera T, Ogata S, Parade M, Brehmer D, Vingron M, Heukamp LC, Buettner R, Zander T, Wolf J, Perner S, Ansen S, Haas SA, Yatabe Y, Thomas RK.	CD74-NRG1 fusions in lung adenocarcinoma.	Cancer Discov	4	415-422	2014

#### IV. 研究成果の刊行物・別刷

## ORIGINAL ARTICLE

# LIM-domain protein AJUBA suppresses malignant mesothelioma cell proliferation via Hippo signaling cascade

I Tanaka<sup>1,2,6</sup>, H Osada<sup>1,3</sup>, M Fujii<sup>1</sup>, A Fukatsu<sup>1,3</sup>, T Hida<sup>4</sup>, Y Horio<sup>4</sup>, Y Kondo<sup>1</sup>, A Sato<sup>5</sup>, Y Hasegawa<sup>2</sup>, T Tsujimura<sup>5</sup> and Y Sekido<sup>1,3</sup>

Malignant mesothelioma (MM) is one of the most aggressive neoplasms usually associated with asbestos exposure and is highly refractory to current therapeutic modalities. MMs show frequent activation of a transcriptional coactivator Yes-associated protein (YAP), which is attributed to the neurofibromatosis type 2 (NF2)–Hippo pathway dysfunction, leading to deregulated cell proliferation and acquisition of a malignant phenotype. However, the whole mechanism of disordered YAP activation in MMs has not yet been well clarified. In the present study, we investigated various components of the NF2–Hippo pathway, and eventually found that MM cells frequently showed downregulation of LIM-domain protein AJUBA, a binding partner of large tumor suppressor type 2 (LATS2), which is one of the last-step kinases of the NF2–Hippo pathway. Although loss of AJUBA expression was independent of the alteration status of other Hippo pathway components, MM cell lines with AJUBA inactivation showed a more dephosphorylated (activated) level of YAP. Immunohistochemical analysis showed frequent downregulation of AJUBA in primary MMs, which was associated with YAP constitutive activation. We found that AJUBA transduction into MM cells significantly suppressed promoter activities of YAP-target genes, and the suppression of YAP activity by AJUBA was remarkably canceled by knockdown of LATS2. In connection with these results, transduction of AJUBA-expressing lentivirus significantly inhibited the proliferation and anchorage-independent growth of the MM cells that harbored ordinary LATS family expression. Taken together, our findings indicate that AJUBA negatively regulates YAP activity through the LATS family, and inactivation of AJUBA is a novel key mechanism in MM cell proliferation.

*Oncogene* advance online publication, 16 December 2013; doi:10.1038/onc.2013.528

**Keywords:** malignant mesothelioma; Hippo pathway; YAP; AJUBA; LATS2

## INTRODUCTION

Malignant mesothelioma (MM), which arises from mesothelial cells, is a highly aggressive human malignancy.<sup>1,2</sup> Global mesothelioma deaths were reported to be about 100 000 in 83 countries by the World Health Organization between 1994 and 2008.<sup>3</sup> MM mortality rates are estimated to increase by 5–10% per year in most industrialized countries until about 2020.<sup>4</sup> Despite intensive treatment with chemotherapy, radiation therapy or surgery, the disease carries a poor prognosis. The median survival time of patients after diagnosis is only 7–12 months.<sup>5–7</sup> MM is usually caused by asbestos exposure, and the latency period after initial exposure is typically longer than 30 years,<sup>8</sup> which connotes accumulation of multiple genetic and epigenetic alterations for MM development.<sup>9</sup> However, the exact molecular pathological process of the development and progression of MM remains obscure.

Around 50% of MM tumors have a genetic mutation of the neurofibromatosis type 2 (NF2) tumor suppressor gene.<sup>10,11</sup> NF2 encodes merlin, a member of the ezrin/radixin/moesin protein family. Merlin is an upstream regulator of the Hippo signaling cascade, which is conserved from *Drosophila* to mammals.<sup>12,13</sup> The Hippo signaling pathway controls organ size through the regulation of cell cycle, proliferation and apoptosis.<sup>14,15</sup> The mammalian components of this pathway include WW

domain-containing protein 1 (WWC1, also called KIBRA), Serine/threonine protein kinase 3 and 4 (STK3 and 4, also called MST2 and 1, orthologs of *Drosophila* Hippo), SAV1, and serine/threonine kinase large tumor suppressor 1 and 2 (LATS1 and 2). Activation of the NF2–Hippo pathway induces the activation of LATS1/2, which phosphorylates and inactivates a transcriptional coactivator, Yes-associated protein (YAP), by translocating YAP from the nucleus to the cytoplasm. The dysfunction of the Hippo pathway, which leads to increased YAP activity with an underphosphorylated form in the nucleus, induces oncogenic transformation owing to activation of transcription factors including TEAD family members.<sup>16</sup> Several target genes of the YAP/TEAD transcriptional complex, including connective tissue growth factor (CTGF) and CCND1 genes, have been shown to be responsible for tumor progression.<sup>12,17,18</sup> We previously reported frequent YAP activation (underphosphorylation) in more than 70% of primary MMs and its pro-oncogenic role in MM cells.<sup>19,20</sup> Besides NF2 mutation, we also found that a subset of MM tumors harbors inactivating mutations of LATS2 and SAV1.<sup>20</sup> Nevertheless, some MM cases without any of these gene alterations still displayed YAP activation, leading us to hypothesize that the other components related to the Hippo pathway might be altered in these cases.

AJUBA family proteins (AJUBA, LIMD1 and WTIP) belong to the Zyxin/AJUBA family, which are components of both

<sup>1</sup>Department of Thoracic Oncology, Aichi Cancer Center Research Institute, Nagoya, Japan; <sup>2</sup>Department of Respiratory Medicine, Nagoya University Graduate School of Medicine, Nagoya, Japan; <sup>3</sup>Department of Cancer Genetics, Program in Function Construction Medicine, Nagoya University Graduate School of Medicine, Nagoya, Japan; <sup>4</sup>Department of Thoracic Oncology, Aichi Cancer Center Hospital, Nagoya, Japan and <sup>5</sup>Department of Pathology, Hyogo College of Medicine, Nishinomiya, Japan. Correspondence: Dr Y Sekido, Division of Molecular Oncology, Aichi Cancer Center Research Institute, Kanokoden 1-1, Chikusa-ku, Nagoya, Aichi 464-8681, Japan. E-mail: ysekido@aichi-cc.jp

<sup>6</sup>Awardee of Research Resident Fellowship from the Foundation for Promotion of Cancer Research.

Received 4 June 2013; Received 22 October 2013; accepted 25 October 2013

integrin-mediated and cell–cell junction adhesive complexes in the capacity of adaptor or scaffold protein.<sup>21</sup> These adaptor or scaffold proteins are known to be crucial regulators of many key signaling pathways, which are involved in cell–cell adhesion, actin cytoskeleton modulation, mitosis, repression of gene transcription, cell differentiation, proliferation and migration.<sup>22,23</sup> Although the mechanisms have not yet been strictly defined, the regulation of their signal pathways is known to be executed by assisting proper localization of signaling components, which include interacting and/or binding with multiple members of signaling pathways, tethering them into complexes.<sup>24,25</sup> In this regard, AJUBA family proteins have been identified to be a binding partner of the LATS family, and the LATS2–AJUBA complex regulates  $\gamma$ -tubulin recruitments involved in mitosis.<sup>26</sup> Recently, Jub (*Drosophila* ortholog of AJUBA family proteins) was shown to activate yorki (*Drosophila* ortholog of YAP) through suppression of the Hippo pathway, and AJUBA family proteins were also found to inhibit YAP phosphorylation in HEK293 and MDCK cells.<sup>27</sup> AJUBA family proteins are thought to be involved in distinct signaling cascades as a multifunctional protein. These studies lead us to hypothesize that AJUBA family proteins might be one of the crucial factors involved in the dysregulation of the Hippo signaling pathway in MM cells.

In this study, using MM cell lines and primary tumors we found that MMs have frequent downregulation of AJUBA, besides the *NF2*, *LATS2* and/or *SAV1* inactivation shown in our previous report.<sup>20</sup> We also found that AJUBA negatively regulates YAP activity through LATS1/2 in MM cells.

## RESULTS

### Frequent reduction of AJUBA expression in MM cell lines

In our previous study, we reported that most MM cell lines harbored either one or two of the *NF2*, *LATS2* and/or *SAV1* gene mutations, which encode major components of the Hippo signaling pathway.<sup>20</sup> The inactivation of these genes leads to the aberrant activation of YAP through decreased phosphorylation of YAP (S127) and more malignant phenotypes of cells.<sup>20</sup> However, there were several MM cell lines that showed YAP activation (underphosphorylation) despite the absence of any of these gene mutations. To determine whether the Hippo signaling pathway inactivation can be caused by alteration of other components, we expanded the analysis of the Hippo signaling pathway including other members in this cascade. Using a panel of 19 of 24 MM cell lines that we previously described<sup>20</sup> and 5 newly established cell lines, we examined the expression status of seven proteins including AJUBA, LIMD1, WTIP, MST1, MST2, LATS1 and KIBRA, which were not characterized in our previous study (Figure 1a and Supplementary Figure S1a). We also reanalyzed the expressions of Merlin, SAV1, LATS2 and YAP, and the phosphorylation status of YAP (S127) (Figure 1a and Supplementary Figure S1a), and confirmed our previous data.<sup>18,20</sup> Although the phosphorylation status of YAP (S127) was different in several cell lines from the previous study, possibly because of the different culture conditions, the overall underphosphorylation status of YAP was consistent, with 21 (85%) of 24 MM cell lines showing YAP activation (Figure 1b).

Interestingly, the expression of AJUBA was significantly reduced in 18 of 24 (75%) MM cell lines (Figure 1a). All six cell lines with intact *NF2*, *SAV1* and *LATS1/2*, including NCI-H28, -H2452, Y-MESO-29, -48, -72 and ACC-MESO-4, showed the downregulation of AJUBA, and four of the six cell lines showed activation (underphosphorylation) of YAP (Supplementary Table 1). Meanwhile, low expression of AJUBA was also observed in 11 of 15 MM cell lines with *NF2* inactivation, and the YAP phosphorylation levels tended to be more reduced in 11 cell lines with AJUBA downregulation (Supplementary Figures S1b and S1c, black columns) compared with four cell lines that retained AJUBA expression (white

columns), although the difference was not statistically significant ( $P=0.057$ ). These results suggested that AJUBA might modulate Hippo signaling while affecting YAP phosphorylation status, and that the alteration of AJUBA expression might be involved in the tumorigenic process of MM. On the other hand, the expression levels of MST1/2 were not decreased in all MM cell lines, and LIMD1, LATS1 and KIBRA were markedly reduced in only three, four and two cell lines, respectively (Figure 1a and Supplementary Figure S1a).

To determine whether AJUBA reduction was caused at the transcriptional level, we carried out real-time reverse transcription–PCR analysis of *AJUBA* together with *WTIP*, *MST1* and *LATS1* (Supplementary Figure S2). Several cell lines with low AJUBA protein expression, including Y-MESO-8D and Y-MESO-29, displayed low *AJUBA* mRNA expressions. However, other low AJUBA protein-expressing cell lines such as ACC-MESO-4 and Y-MESO-9 did not show *AJUBA* mRNA downregulation. These results suggested that the reduction of AJUBA in MM cells is induced either at the transcriptional or at the post-transcriptional levels.

Regarding WTIP, several cell lines showed relatively weak WTIP expression in western blot analysis, but, due to a possible low specificity of the antibody (discussed below in Supplementary Figure S3), we also conducted real-time reverse transcription–PCR analysis and found several cell lines with low expressers of *WTIP* (Supplementary Figure S2).

### AJUBA is associated with increased YAP phosphorylation in MM cells

To determine whether AJUBA downregulation is involved in the Hippo signaling dysregulation in MM cells, we studied three MM cell lines with low AJUBA expression, including NCI-H290, Y-MESO-8D and NCI-H28 (Supplementary Table 1, indicated in pink in the cell line names). NCI-H290 and Y-MESO-8D cell lines with *NF2* mutation showed YAP activation (underphosphorylation), whereas the other components of the Hippo pathway were intact. NCI-H28 had intact *NF2* and the Hippo pathways, but YAP phosphorylation was moderately activated.

Using these cell lines with low AJUBA expression, we transduced AJUBA-expressing lentivirus and studied the changes in YAP phosphorylation status. Surprisingly, we found that exogenous AJUBA markedly led to an increase in YAP phosphorylation levels in all three cell lines (Figures 2a and b), which seemed to be contrary to the result in the previous report on *Drosophila*—that is, dJub dephosphorylates Yorkie.<sup>27</sup> To exclude a possibility that ectopically expressed AJUBA was too abundant and caused this unexpected result, we also compared AJUBA overexpression levels in the three AJUBA-transduced cell lines with endogenous AJUBA expression levels in MeT-5A, and in two AJUBA-unsuppressed MM cell lines, MSTO-211H and Y-MESO-43 (Supplementary Figures S2b and S2c). We found that the transduced AJUBA expression levels were about threefold higher than the endogenous basal levels, which seemed to be acceptable levels for *in vitro* functional assays.

To confirm whether or not YAP phosphorylation induced by AJUBA transduction affects the expression of transcriptional targets of YAP, we studied *CCND1*, one of the YAP-target genes, and found a decrease in *CCND1* protein expression in all three cell lines (Figure 2a). Furthermore, dual-luciferase assay using the promoter reporters of the *CCND1* and *CTGF* genes, the latter being another known YAP target,<sup>18</sup> clearly demonstrated that exogenous AJUBA markedly suppressed both promoter activities (Figures 2c and d). Conversely, RNA interference-mediated silencing of endogenous AJUBA led to the decrease in YAP phosphorylation levels in MeT-5A and Y-MESO-43 cells with ordinary expression of all three AJUBA family proteins (Supplementary Figures S3a and S3b). Likewise, AJUBA small interfering RNA transduction in MeT-5A cells increased both *CCND1* and *CTGF* promoter activities, indicating that



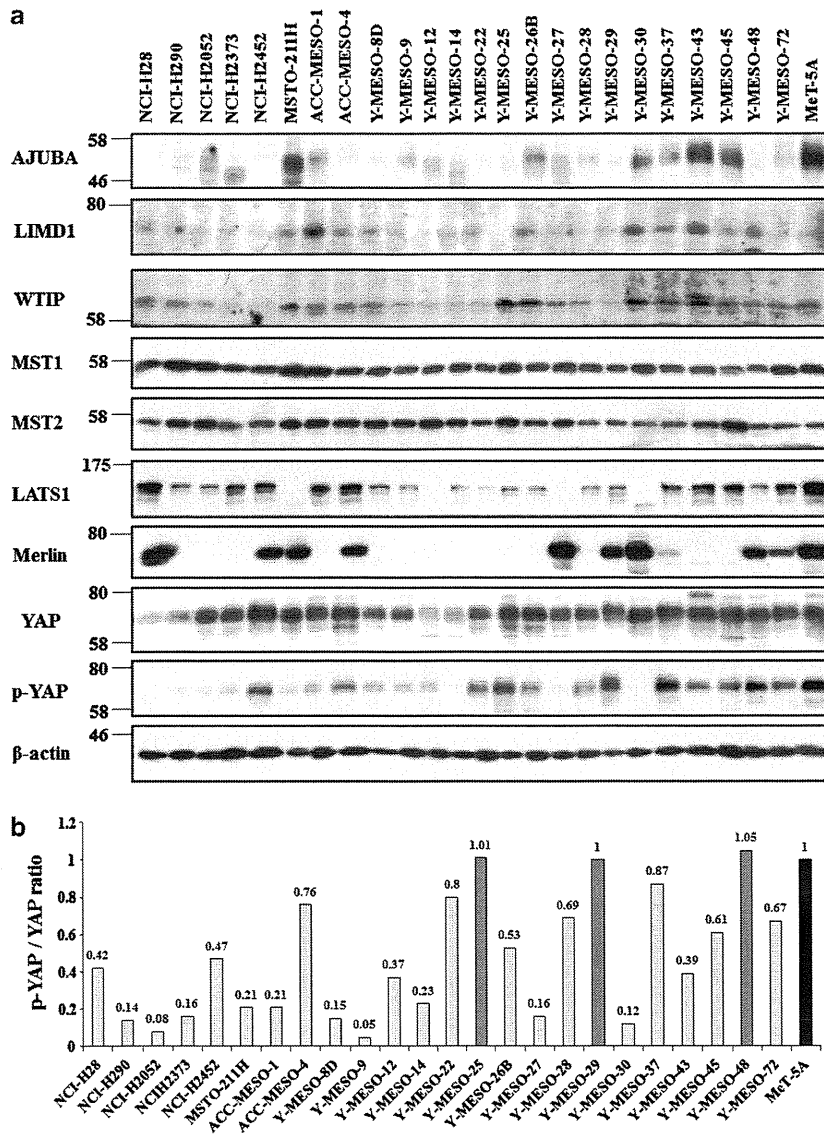


**Figure 1.** Expression analysis of the Hippo pathway components in MM cell lines. **(a)** Western blot analysis of AJUBA, LIMD1, WTIP, MST1, MST2, LATS1, Merlin, YAP and phospho-YAP Ser127 (p-YAP). AJUBA expression was undetectable in 15 and significantly low in 3 of 24 MM cell lines compared with an immortalized normal mesothelial cell line MeT-5A (also see Supplementary Table 1). Expression levels of LIMD1 or LATS1 were significantly reduced in 3 or 4 MM cell lines, respectively. No reduction of MST1 and MST2 was observed in any MM cell line. Merlin (*NF2* gene product) expression was undetectable in 14 and significantly low in one of 24 MM cell lines, compared with MeT-5A cells. YAP phosphorylation level was remarkably reduced in 21 of 24 MM cell lines compared with MeT-5A. Expression of  $\beta$ -actin was used as the control. **(b)** p-YAP and YAP signals shown in **a** were measured and the intensity ratios were shown with a bar graph with reference to MeT-5A. Lower p-YAP/YAP value indicates higher YAP activation status.

endogenous AJUBA also regulates YAP-target gene transcription (Supplementary Figure S3c). In contrast, silencing of endogenous WTIP increased YAP phosphorylation levels in both MeT-5A and Y-MESO-43 cells (Supplementary Figures S3a and S3b). Expression of WTIP small interfering RNA was also assessed at the mRNA level, because western blot analysis did not sufficiently confirm the effect of small interfering RNA knockdown (Supplementary Figure S3d).

AJUBA indirectly induces YAP phosphorylation via the LATS family. To determine whether YAP phosphorylation induced by AJUBA transduction is dependent on the Hippo signaling cascade, we transduced AJUBA into two MM cell lines, Y-MESO-14 and Y-MESO-27, which harbored *LATS2* homozygous deletion.<sup>20</sup> As YAP is directly phosphorylated by LATS1 or LATS2, and these two cell lines showed different LATS1 status (Y-MESO-14 had it, but

Y-MESO-27 had lost LATS1 expression), we considered that these cell lines were useful for vigorous examination of a possible LATS family effect on AJUBA (Figure 3a).

After AJUBA transduction, the YAP phosphorylation level was slightly increased in Y-MESO-14 cells with LATS1 expression, whereas Y-MESO-27 cells without LATS1 expression did not show any change in the YAP phosphorylation level (Figures 3a and b). The dual-luciferase reporter assay also confirmed that AJUBA transduction suppressed neither the activity of *CCND1* nor that of the *CTGF* promoter in Y-MESO-27 cells (Figure 3c). These results indicated that AJUBA induces YAP phosphorylation via LATS1/2 in MM cells.

To further confirm these results, we conducted knockdown of LATS1 or LATS2 in NCI-H290 and Y-MESO-8D cell lines, both having intact LATS1/2, after infection of AJUBA-expressing lentivirus. Interestingly, LATS2 knockdown significantly suppressed YAP phosphorylation induced by exogenous AJUBA in both cell lines,

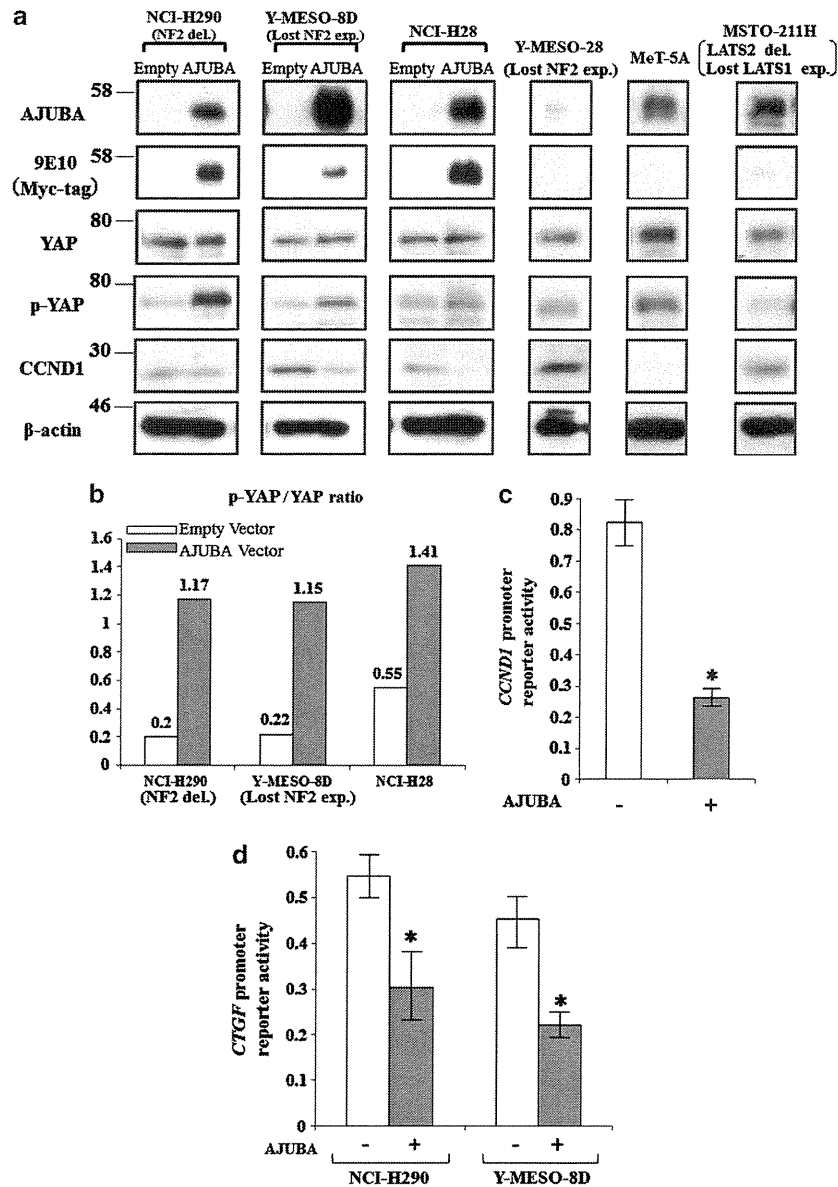


**Figure 2.** AJUBA is associated with an increased YAP phosphorylation level. **(a)** Western blot analyses. NCI-H290, Y-MESO-8D and NCI-H28 cells were infected with AJUBA-expressing or empty lentivirus. AJUBA transduction led to a marked increase in YAP phosphorylation levels and to a decrease in CCND1 expression levels in these three cell lines. Ectopically expressed AJUBA and subsequent effects on YAP and CCND1 were compared with the patterns in another three cell lines. Y-MESO-28, another representative AJUBA-low cell line, showed a phospho-YAP-low and CCND1-high pattern, whereas MeT-5A expressing ordinary level of AJUBA showed a phospho-YAP-high and CCND1-low pattern; these patterns were similar to the results of empty and AJUBA transduction in the three cell lines. Meanwhile, MSTO-211H also expressed AJUBA as abundantly as MeT-5A, but showed high-CCND1 expression compared with MeT-5A, because of its *LATS2* deletion and low-*LATS1* expression. **(b)** p-YAP and YAP signals shown in **a** were measured, and the intensity ratios were indicated with a bar graph. **(c)** *CCND1* promoter reporter assay. *CCND1* promoter reporter construct was transfected into NCI-H290 cells together with an AJUBA-expressing vector, pcDNA3-AJUBA, or empty vector. AJUBA markedly suppressed the *CCND1* promoter activity. **(d)** *CTGF* promoter reporter assay. *CTGF* promoter reporter construct was transfected into NCI-H290 and Y-MESO-8D cells together with pcDNA3-AJUBA, or empty vector. AJUBA significantly suppressed the *CTGF* promoter activity in both cell lines. Average and s.d. of triplicated experiments are demonstrated in **c** and **d**. \* $P < 0.05$  versus empty vector control. del., deletion; exp., expression.

whereas *LATS1* knockdown showed only moderate suppression (Figures 3d and e). Furthermore, dual-luciferase assays showed that *LATS2* knockdown in NCI-H290 cells effectively recovered the *CCND1* promoter activity that was suppressed by AJUBA (Figure 3f). Similarly, *LATS2* knockdown effectively recovered the *CTGF* promoter activity that was attenuated by AJUBA, whereas *LATS1* knockdown showed only a marginal effect (Figure 3g and Supplementary Figure S3e). These results indicated that AJUBA led to increased YAP phosphorylation and inhibited the

transcriptional coactivity of YAP through the *LATS* family, and that its effect seemed to be relatively more dependent on *LATS2* than on *LATS1*.

AJUBA mainly localizes in the MM cell cytoplasm and translocates YAP

YAP, when phosphorylated, is known to translocate from the nucleus to the cytoplasm.<sup>28</sup> To investigate whether AJUBA is also

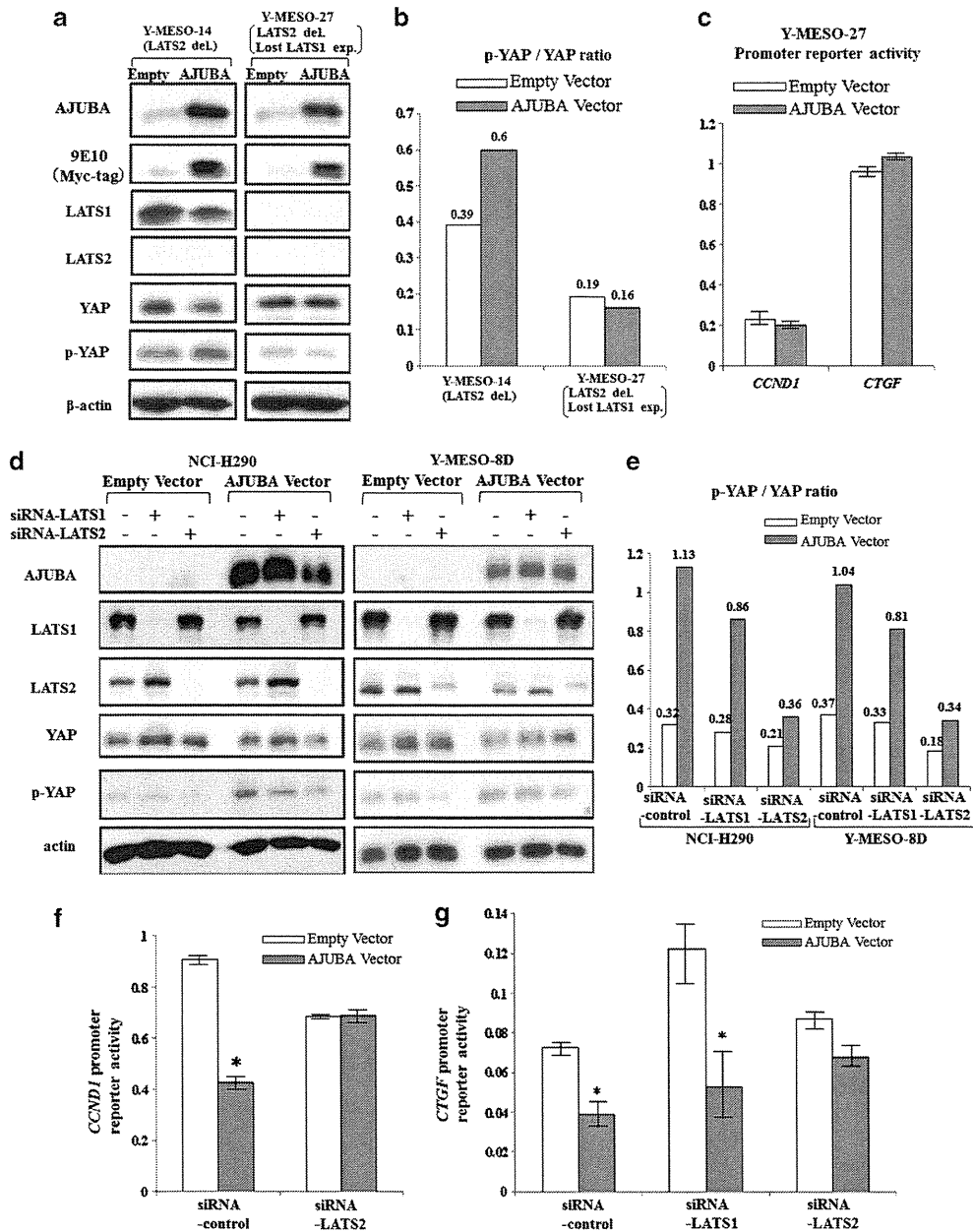


**Figure 3.** AJUBA indirectly increases YAP phosphorylation level through LATS family. **(a)** Y-MESO-14 and Y-MESO-27 cells harboring *LATS2* homozygous deletion were infected with Myc-tagged AJUBA-expressing or empty lentivirus. Western blot analysis demonstrated that exogenous AJUBA led to a slight increase in the YAP phosphorylation level in Y-MESO-14 cells with ordinary *LATS1* expression, but not in Y-MESO-27 cells, which had simultaneous downregulation of *LATS1*. **(b)** p-YAP and YAP signals presented in **a** were measured and indicated with a bar graph as p-YAP/YAP ratio. **(c)** Promoter reporter assays. *CCND1* or *CTGF* promoter reporter construct was transfected into Y-MESO-27 cells with both *LATS1* and *LATS2* inactivation. AJUBA co-transduction did not affect either of the two promoter activities. **(d)** After infection of AJUBA-expressing or empty lentivirus, small interfering RNA-induced knockdown of *LATS1* or *LATS2* was conducted using NCI-H290 and Y-MESO-8D cells. *LATS2* knockdown effectively, but *LATS1* knockdown only slightly, suppressed phospho-YAP levels, despite AJUBA transduction. **(e)** p-YAP and YAP signals shown in **d** are indicated with a bar graph of p-YAP/YAP ratio. **(f)** *CCND1* promoter reporter assay using NCI-H290 cells. After transfection of the *CCND1* promoter reporter together with AJUBA-expressing vector (or empty vector), small interfering RNA against *LATS2* was transfected, and then dual-luciferase reporter assay was conducted. Suppression of *CCND1* promoter activity by AJUBA was canceled by *LATS2* knockdown. **(g)** *CTGF* promoter reporter assay. After transfection of the *CTGF* promoter reporter with AJUBA-expressing vector (or empty vector) into Y-MESO-8D cells, the small interfering RNA against *LATS1* or *LATS2* was transfected, and then dual-luciferase reporter assay was conducted. AJUBA markedly suppressed the activity of *CTGF* promoter, and *LATS2* knockdown effectively, but *LATS1* knockdown only marginally, attenuated the suppression of *CTGF* promoter activity by AJUBA. Average and s.d. of triplicated experiments are demonstrated in **c**, **f** and **g**. \* $P < 0.05$  versus small interfering RNA control.

associated with YAP translocation in MM cells, we performed a cell fractionation experiment using two MM cell lines after AJUBA transduction. Western blot analysis of nuclear and cytoplasmic fractions of the transfectants showed that exogenous AJUBA was mainly expressed in the cytoplasmic fraction and that YAP was

phospho-YAP (Ser127) levels were significantly increased in the cytoplasm in both cell lines (Figures 4a and b).

Next, we performed immunofluorescent analysis to confirm the subcellular localization for exogenously expressed AJUBA in Y-MESO-8D cells and for endogenous AJUBA in MeT-5A cells. The results

showed that both exogenous and endogenous AJUBA were mainly localized in the cytoplasm (Figure 4c and Supplementary Figure S3f). AJUBA transduction led to a clear increase in the YAP phosphorylation level in Y-MESO-8D cells, which was associated with an increased YAP expression level in the cytoplasm (Figure 4c). These results suggested that AJUBA suppressed YAP activity through phosphorylation and its cytoplasmic translocation in MM cells.

#### AJUBA inhibits cell growth of MM cell lines dependent on LATS status

To verify whether AJUBA has a growth-suppressive activity against MM cells, we carried out a cell proliferation assay. As expected,

AJUBA transduction significantly inhibited cell proliferation of all three MM cell lines, NCI-H28, NCI-H290 and Y-MESO-8D, which retained both LATS1 and LATS2 expression (Figure 5a). In contrast, such significant suppression of cell proliferation was not observed in two MM cell lines, Y-MESO-14 and Y-MESO-27, which harbored *LATS2* deletion (Supplementary Figure S4a). However, there still appeared to be a difference in the proliferation curves between the latter two cell lines; AJUBA still induced a weak suppression of Y-MESO-14 cells, which retained LATS1, but not of Y-MESO-27 without LATS1 expression (Supplementary Figure S4a). The suppression levels in each MM cell line were well consistent with the YAP phosphorylation status induced by AJUBA (Figures 2a and 4a).

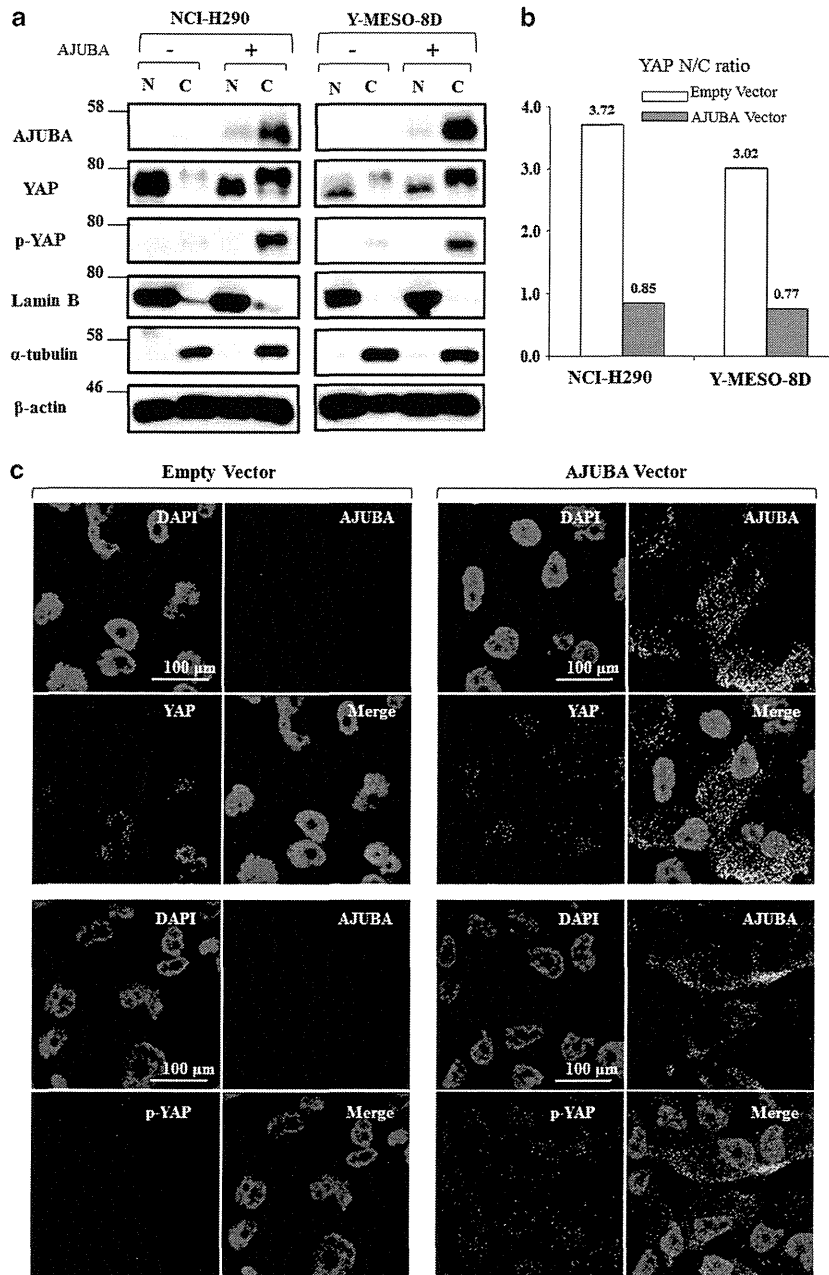


**Figure 4.** Subcellular localization of AJUBA and YAP. (a) Western blot analysis. NCI-H290 and Y-MESO-8D cells were infected with AJUBA-expressing or empty lentivirus and fractionated into nuclear and cytoplasmic fractions. AJUBA was mainly localized in the cytoplasm, and AJUBA induced a significant increase in YAP and phospho-YAP (Ser127) levels in the cytoplasm. (b) Nucleus/cytoplasm ratio (N/C ratio) of YAP shown in a is indicated with a bar graph. (c) Immunofluorescent microscopic analysis of Y-MESO-8D cells. Exogenous AJUBA was mainly localized in the cytoplasm of Y-MESO-8D cells infected with AJUBA-expressing lentivirus. Exogenous AJUBA induced a marked increase in total YAP and YAP phosphorylation in the cytoplasm.

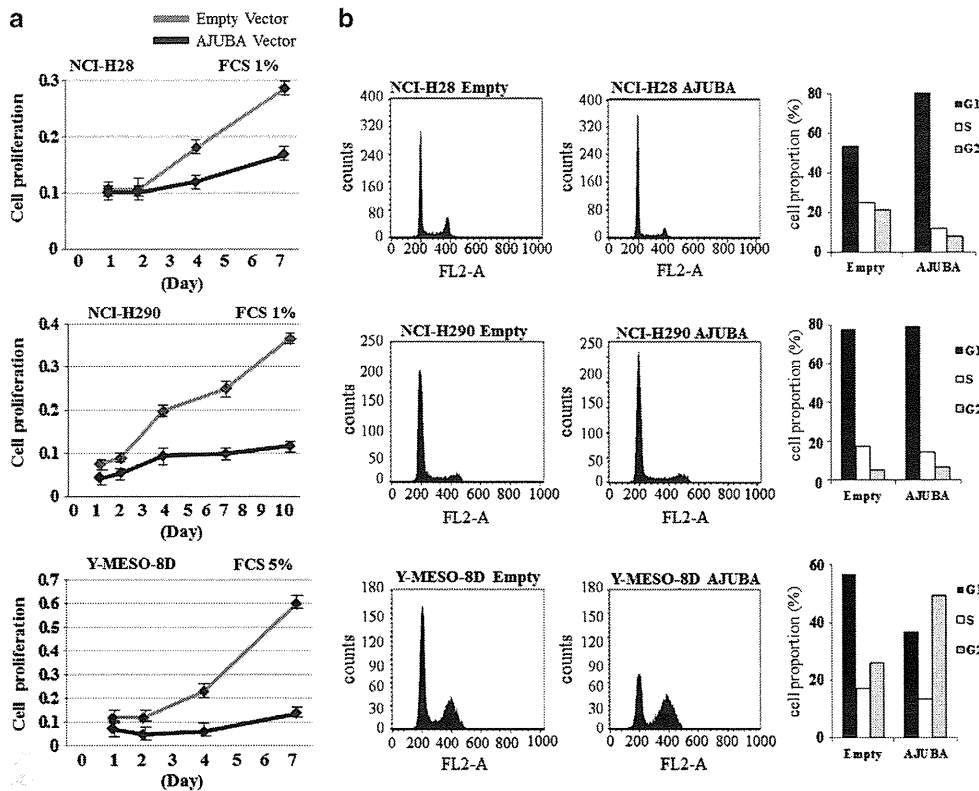


**Figure 5.** AJUBA inhibits cell proliferation of MM cell lines. **(a)** Cell proliferation assays. After infection with AJUBA-expressing or empty lentivirus, calorimetric assays were performed at each point. AJUBA transduction significantly inhibited the cell proliferation of NCI-H28 and NCI-H290 cells in the low-serum condition with 1% FCS and of Y-MESO-8D cells in the usual condition at 5% FCS. **(b)** Flow cytometric analyses. AJUBA transduction significantly increased cell population of G1 phase and decreased the population of S phase in NCI-H28 and NCI-H290 cells, indicating G1 arrest as an early response. Y-MESO-8D cells exhibited remarkably increased cell population of G2 phase and decreased population of S-phase, indicating G2 arrest. Average and s.d. of triplicated experiments are demonstrated in **a**.

Furthermore, we studied cell cycle profiles to elucidate the possible suppressive mechanisms of MM cell proliferation by AJUBA. Flow cytometric analyses demonstrated that the cell population of G1 phase increased, whereas that of S phase decreased, in NCI-H28 and NCI-H290 cells after infection of AJUBA-expressing lentivirus (Figure 5b). These results indicated that G1 cell cycle arrest was induced in both cell lines by exogenous AJUBA, which was consistent with the result of YAP knockdown in our previous report.<sup>18</sup> In contrast, Y-MESO-8D cells displayed decreased S phase and clearly increased G2 phase-cell population, suggesting that exogenous AJUBA induced G2 cell cycle arrest in this cell line. Thus, it was considered that AJUBA can induce cell cycle arrest in either G1 or G2 phase in MM cells with intact LATS1/2. Consistent with these data, LATS1 or LATS2 knockdown led to the recovery of cell proliferation in NCI-H290 cells transfected with AJUBA-expressing vector (Supplementary Figures S4c and S4d). Meanwhile, Y-MESO-14 and Y-MESO-27 cells with LATS2 deletion showed little or no change in cell populations in each cell cycle, which well accorded with marginal or no suppression of cell proliferation of these cell lines after AJUBA transduction (Supplementary Figure S4b).

We also carried out a soft agar colony formation assay. AJUBA transduction caused marked reduction in the number and size of colonies of NCI-H290 and Y-MESO-8D cells, indicating that AJUBA significantly decreased anchorage-independent growth in the presence of the LATS family (Figures 6a and b). On the other hand, similar to the results of the cell proliferation assay, AJUBA transduction induced weak or no effect on Y-MESO-14 and Y-MESO-27 cell lines, respectively.

Immunohistochemical analysis of AJUBA and YAP in primary MMs To examine whether the frequent inactivation of AJUBA detected in MM cell lines is observed also in primary MM specimens, we carried out immunohistochemical analysis with an anti-AJUBA antibody. Among 20 cases, 5 (25%) showed negative (0) and 11 (55%) showed weak (1+) staining of AJUBA, whereas only 4 cases showed strong (2+) staining, indicating that AJUBA expression was frequently and consistently reduced in both MM cell lines and primary MM specimens (16 (80%); negative or weak) (Figure 7a and Supplementary Table 2). Consistent with the above results, immunohistochemical analysis also confirmed that AJUBA was mainly localized in the cytoplasm in all AJUBA-positive cases (Figure 7b).

To determine whether AJUBA downregulation is associated with YAP activation in primary MMs, we next performed immunohistochemical analysis of YAP. Among 20 cases, 13 (65%) showed that YAP was stained more strongly in the nucleus than in the cytoplasm, indicating constitutive activation of YAP (Figures 7a and b). Quite consistent with the *in vitro* results, all five cases of AJUBA-negative cases (Figure 7a and indicated in blue in Supplementary Table 2) exhibited nuclear localization of YAP, suggesting the association of AJUBA inactivation with YAP activation in primary MMs (Figures 7a and b).

## DISCUSSION

In the present study, we found that AJUBA is frequently downregulated in MM cells and acts as a tumor suppressor by inducing YAP phosphorylation in a LATS family-dependent

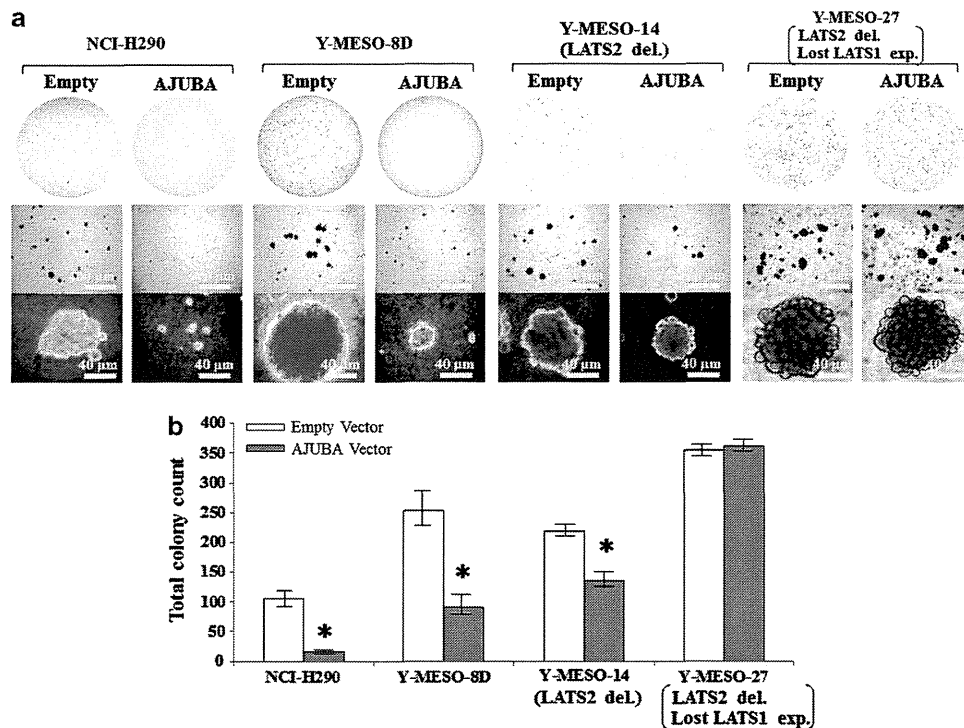


**Figure 6.** AJUBA suppresses anchorage-independent colony formation in MM cells. **(a)** Soft agar colony formation assays with AJUBA transduction. After 12-day incubation, colonies were stained with 0.03% crystal violet. Low (top), medium (middle) and high magnification (bottom) photos show that anchorage-independent growth was significantly suppressed in NCI-H290 and Y-MESO-8D cell lines. The size and number of colonies in the Y-MESO-14 cell line with lost LATS2 expression were moderately reduced, but not at all in the Y-MESO-27 cell line, which harbored *LATS2* deletion and low-LATS1 expression. **(b)** A graphic presentation of the soft agar colony formation assays of **a**. Average and s.d. of triplicated experiments are demonstrated in **b**. \* $P < 0.05$  versus empty lentivirus control.

manner. Although the components of the Hippo pathway between *Drosophila* and mammals are highly conserved, our study demonstrates that AJUBA attenuates YAP activity in human MM cell lines, which contradicts its possible pro-oncogenic function in *Drosophila*, HEK293 cells and canine kidney MDCK cells.<sup>27</sup> In this regard, it is worth noting that RAS association domain family (RASSF) members, which are also known to be involved in the Hippo signaling pathway, regulate this pathway in opposite ways between *Drosophila* and mammals.<sup>29,30</sup> Furthermore, in preimplantation embryos, the Hippo signaling pathway was also shown to control cell differentiation,<sup>31</sup> although the Hippo pathway regulates cell proliferation by contact inhibition in cultured cells. Therefore, the tumor-suppressive function of AJUBA that we found in this study might be attributable to the evolutionary distance of gene functions and/or to the difference in cell lineage or germ layer for example, the mesothelium originates from the mesoderm.

We previously reported that the frequencies of alterations of *NF2* and *LATS2* expression in MM cell lines were about 50% and 20%, respectively.<sup>20</sup> However, there were several MM cell lines with YAP activation regardless of the absence of *NF2* or *LATS2* alteration. The present study revealed that all six cell lines without *NF2* or *LATS1/2* alterations showed the downregulation of AJUBA (Supplementary Table 1), suggesting that AJUBA inactivation is involved in the regulation of Hippo signaling activity. In total, 21 of 24 cell lines with YAP activation showed at least one alteration among *NF2*, *LATS1/2* and AJUBA. Individual cell lines showed obvious single or multiple alterations of Hippo components. The difference in the target molecules also seemed to influence the levels of YAP activity. For instance, MM cells with only *NF2* inactivation showed relatively modest YAP activation (Supplementary Table 1 and Supplementary Figure S1b). This

may suggest that *NF2* inactivation may not be sufficient to fully activate YAP, and thus *NF2*-defective MM cell lines frequently acquire additional alterations of other molecules such as *SAV1*, *KIBRA*, *LATS1/2* or *AJUBA* that lead to the enhancement of YAP activation (Supplementary Figures S1b and S1c). In contrast, the *LATS1/2* alteration completely disrupts the last step of the Hippo signaling cascade, resulting in significant reduction of YAP phosphorylation. Indeed, three MM cell lines with *LATS1/2* inactivation but without *NF2* mutation had most activated (underphosphorylated) YAP (Supplementary Figure S1b, red columns).

Our study indicates the difference between LATS1 and LATS2 in the regulation of YAP under exogenous AJUBA transduction. Compared with three cell lines with intact *LATS1/2* (Figure 2a), AJUBA transduction induced only a modest effect on YAP phosphorylation in the Y-MESO-14 cells with *LATS2* deletion and no effect in the Y-MESO-27 cells with both *LATS1* and *LATS2* inactivation (Figure 3a). These results were well consistent with the weaker suppression of cell proliferation and colony formation by AJUBA transduction in these cell lines (Figure 6 and Supplementary Figure S4a). Furthermore, in the MM cell lines with intact *LATS1/2* that were transfected with AJUBA-expressing vector, *LATS2* knockdown decreased a phosphorylated form of YAP more than did *LATS1* knockdown, suggesting that *LATS2* may have a more significant role. However, the effect of *LATS1* knockdown could be underestimated, because silencing *LATS1* resulted in increased *LATS2* protein, which might enhance the difference in the effects between knockdown of *LATS1* and *LATS2* (Figure 3d). Thus, the possible association and stimulation mechanism between AJUBA, *LATS1/2* and YAP need to be more vigorously investigated in a future study to elucidate the exact role of *LATS1* on the Hippo signaling regulation. Finally, as the MM

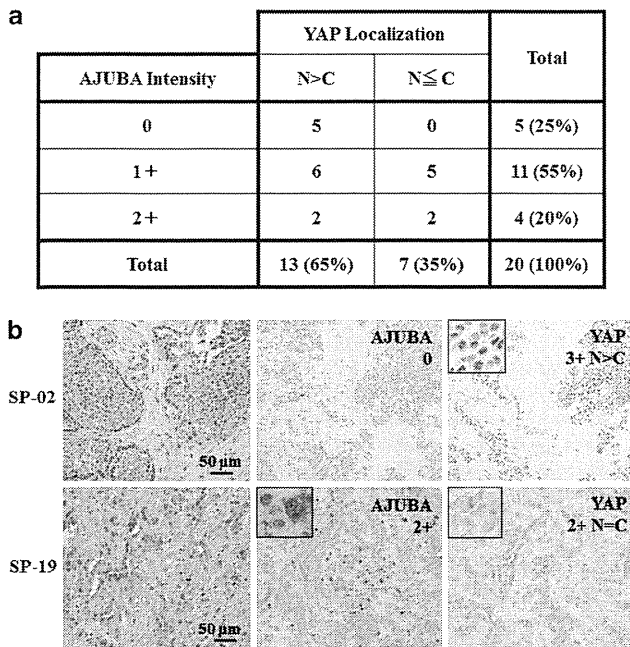


**Figure 7.** Immunohistochemical analyses of AJUBA and YAP in 20 primary MMs. **(a)** Twenty primary MM specimens were stained with anti-AJUBA and anti-YAP antibodies and were classified according to the YAP localization pattern (N>C or N≤C) and the staining intensity of AJUBA (negative (0), weak (1+) or strong (2+)). All 5 AJUBA-negative cases showed the nuclear localization pattern (N>C) of YAP protein. N, nucleus; C, cytoplasm. **(b)** AJUBA and YAP staining patterns of two representative cases are demonstrated. Specimen-02 showed no AJUBA expression (0) and strong nuclear staining of YAP (3+, N>C). Meanwhile, Specimen-19 had strong AJUBA expression (2+) and YAP staining in both the nucleus and the cytoplasm (2+, N=C).

cells with both LATS1 and LATS2 inactivation showed the most underphosphorylated YAP, the alteration of both LATS1 and LATS2 may be a crucial event apart from the *NF2* loss in the development of MM.

We studied the effects of AJUBA family proteins on YAP activation using the small interfering RNAs against AJUBA, LIMD1 and WTIP in the MeT-5A and Y-MESO-43 cell lines (Supplementary Figures S3a and S3b). We found that AJUBA knockdown reduced the YAP phosphorylation level, whereas LIMD1- or WTIP-knockdown led to an increase in the YAP phosphorylation level, suggesting that LIMD1 and WTIP might negatively regulate the Hippo signaling pathway, which was consistent with the previous report.<sup>27</sup> Moreover, in the Y-MESO-43 cell line, LIMD1- or WTIP- knockdown caused a decrease in the AJUBA expression level, by which a reduction in YAP phosphorylation levels could have been expected. However, despite the subsequent AJUBA downregulation, the YAP phosphorylation level was instead increased in this LIMD1- or WTIP-knockdown cell line. These data possibly suggest contrasting effects among AJUBA family proteins—that is, LIMD1/WTIP might counteract AJUBA and activate YAP in the MM cells. However, further studies are definitely needed to clarify the functional interactions among AJUBA family proteins on the Hippo signaling pathway in MM cells.

We found that overexpressed AJUBA induces either G1/S or G2/M arrest in MM cells. We previously reported that *FOXM1* was one of the target genes of YAP/TEAD and that YAP knockdown induces downregulation of *FOXM1*.<sup>18</sup> As *FOXM1* is known to regulate the

transcription of cell cycle-specific genes that are responsible in both G1/S and/or G2/M transition,<sup>32–37</sup> the cell cycle arrest induced by AJUBA might be due to *FOXM1* downregulation. Interestingly, Y-MESO-8D cells predominantly presented G2 arrest induced by AJUBA. This result was consistent with a finding that the dual-luciferase reporter assay did not show a reduction of *CCND1* promoter activity in the Y-MESO-8D cell line (data not shown), suggesting that Y-MESO-8D cells have low dependency on *CCND1* in G1/S progression. In addition, AJUBA has been shown to interact with multiple factors such as Aurora A, Aurora B and BUBR1.<sup>38,39</sup> This indicates that G2 arrest in this cell line was related to the involvement of AJUBA at the G2/M checkpoint with binding Aurora A.<sup>38,40</sup>

Recently, the activity of Hippo-YAP has been shown to be regulated by various factors—for example, protease-activated receptors and G-protein-coupled receptor signaling.<sup>41,42</sup> Mechanical signals, for example, cytoskeleton organization, cell attachment, intercellular junction and cell morphology, have also been suggested to be involved in the Hippo-YAP regulation.<sup>43–46</sup> In this regard, AJUBA was shown to directly interact with both  $\alpha$ -catenin and F-actin, which were recruited at an adherent junction.<sup>47</sup> Thus, AJUBA might be involved in the signal transduction from mechanical signals to YAP activity, and might modulate the proliferation status of cells.

In this study, we found frequent inactivation of AJUBA in MM as well as its tumor-suppressive role that is associated with the Hippo signaling pathway. Although most MM cells show the Hippo pathway inactivation leading to constitutive activation of YAP, new treatment strategies to target this pathway may well be developed to cure patients with this highly aggressive malignancy.

## MATERIALS AND METHODS

### Cell lines

Eighteen Japanese MM cell lines including ACC-MESO-1, -4, Y-MESO-8D, -9, -12, -14, -22, -25, -26B, -27, -28, -29, -30, -37, -43, -45, -48 and -72 were established in our laboratory, and cells at 10–15 passages were used for each assay. Four MM cell lines including NCI-H28, NCI-H2052, NCI-H2373 and MSTO-211H, and one immortalized mesothelial cell line, MeT-5A, were purchased from the American Type Culture Collection (Rockville, MD, USA), and then used at 3–5 passages after reception. Two MM cell lines, NCI-H290 and NCI-H2452, were the kind gift of Dr Adi F Gazdar. All MM cell lines and MeT-5A were cultured in RPMI-1640 medium supplemented with 10% fetal calf serum (FCS) and 1 $\times$  antibiotic-antimycotic Invitrogen (Carlsbad, CA, USA) at 37 °C in a humidified incubator with 5% CO<sub>2</sub>.

### Expression constructs and reagents

AJUBA-expressing plasmid and lentiviral vectors were constructed with pcDNA3 with Myc-tag vector (Invitrogen) or CSII-CMV-MCS-IRES2-Blasticidin vector (provided by Dr H Miyoshi, RIKEN BioResource Center). The wild-type AJUBA was amplified with cDNA synthesized from MeT-5A RNA, by reverse transcription-PCR using Pfu-Turbo DNA polymerase (Agilent Technologies, Tokyo, Japan) or PrimeSTAR Max DNA polymerase (Takara Bio, Otsu, Japan). Oligonucleotides were designed within the *AJUBA* open reading frame (*AJUBA*, 5'-ATGGAGCGGTTAGGAGAGAAAGC-3' and 5'-TCAGATATAGTTGGCAGGGGTTGT-3'). For luciferase reporter plasmids, *CCND1* and *CTGF* were amplified and cloned into pGL3 basic luciferase reporter vector (Promega, Madison, WI, USA) as described previously.<sup>18,48</sup> Rabbit anti-YAP antibody (EP1674Y) was purchased from Abcam (Tokyo, Japan). Rabbit anti-phospho-YAP (S127) antibody (#4911), anti-LATS1 antibody (#9153), anti-MST1 antibody (#3682), anti-MST2 antibody (#3952), anti-Merlin antibody (#6995), anti-AJUBA antibody (#4897) and mouse anti-*CCND1* antibody (#2926) were from Cell Signaling Technology (Danvers, MA, USA). Mouse anti-AJUBA antibody (sc-374610) and anti-c-Myc antibody (sc-40), anti- $\alpha$ -tubulin antibody (sc-5286), goat anti-LIMD1 antibody (sc-55845) and anti-WTIP antibody (sc-24173) were from Santa Cruz (Santa Cruz, CA, USA). Mouse anti-LATS2 antibody (MAB0019) was from Abnova Corporation (Taipei, Taiwan). Rabbit anti-WWC1 (KIBRA)

antibody (HPA038016) and mouse anti- $\beta$ -actin (A5441) were from Sigma (St Louis, MO, USA).

#### Transfection of siRNA

AJUBA, LIMD1, WTIP, LATS1, LATS2 and control small interfering RNAs (ON-TARGETplus SMARTpool siRNA reagent, Thermo Fisher Scientific, Lafayette, CO, USA) were introduced into cells by transient transfection with RNAi MAX (Invitrogen) in accordance with the manufacturer's instructions.

#### Cell proliferation assay

MM cells ( $1 \times 10^4$ ) were seeded on flat-bottomed 24-well plates. After 24 h, cells were transduced with lentiviral vectors, and then incubated for an additional 48 h. Cells were incubated to grow for an additional 5 days under Blastocidin (InvivoGen, San Diego, CA, USA) selection. The medium was then changed with fresh RPMI-1640 medium with 1% FCS as described previously.<sup>19</sup> As an exceptional case, Y-MESO-8D cells were cultured in fresh RPMI-1640 medium with 5% FCS because this cell line hardly grew in the 1% FCS medium. After an additional 24 h incubation, calorimetric assays were performed by adding 30  $\mu$ l of Tetra Color One (Seikagaku, Tokyo, Japan) containing 2-(2-methoxy-4-nitrophenyl)-3-(4-nitrophenyl)-5-(2,4-disulfo phenyl)-2H-tetrazolium, monosodium salt and 1-methoxy-5-methylphenyl methylsulfate as electron carrier in each well and incubated at 37 °C for 1 h. Absorbance was measured at 450 nm using a multiplate reader. Cell proliferation was shown as a relative ratio to control cells.

#### Anchorage-independent growth in soft agar

Bottom agar was made of 1.5 ml of 0.5% agar supplemented with 10% FCS and RPMI-1640 medium, plated in 35 mm plates. Cells ( $3.0 \times 10^4$ ) were mixed with 1.0 ml of 0.35% agar supplemented with 10% FCS and RPMI-1640 medium, and then added onto the bottom agar. Cells were incubated to grow and form colonies for 12 days. Colonies were stained with 0.03% crystal violet, and the numbers of colonies were counted.

#### CONFLICT OF INTEREST

The authors declare no conflict of interest.

#### ACKNOWLEDGEMENTS

This work was supported in part by KAKENHI (24650650, 25290053), Grants-in-Aid for Third-Term Comprehensive Control Research for Cancer from the Ministry of Health, Labor and Welfare of Japan, P-DIRECT and the Takeda Science Foundation (YS). We thank Dr Adi F Gazdar for the cell lines and Mari Kizuki and Miwako Nishizawa for their excellent technical assistance. IT was supported by the Foundation for Promotion of Cancer Research.

#### REFERENCES

- Pass HI, Vogelzang N, Hahn S, Carbone M. Malignant pleural mesothelioma. *Curr Probl Cancer* 2004; **28**: 93–174.
- Yang H, Testa JR, Carbone M. Mesothelioma epidemiology, carcinogenesis, and pathogenesis. *Curr Treat Options Oncol* 2008; **9**: 147–157.
- Delgermaa V, Takahashi K, Park EK, Le GV, Hara T, Sorahan T *et al*. Global mesothelioma deaths reported to the World Health Organization between 1994 and 2008. *Bull World Health Organ* 2011; **89**: 716–724.
- Carbone M, Ly BH, Dodson RF, Pagano I, Morris PT, Dogan UA *et al*. Malignant mesothelioma: facts, myths, and hypotheses. *J Cell Physiol* 2012; **227**: 44–58.
- Robinson BW, Lake RA. Advances in malignant mesothelioma. *N Engl J Med* 2005; **353**: 1591–1603.
- Robinson BW, Musk AW, Lake RA. Malignant mesothelioma. *Lancet* 2005; **366**: 397–408.
- Vogelzang NJ, Rusthoven JJ, Symanowski J, Denham C, Kaukel E, Ruffie P *et al*. Phase III study of pemetrexed in combination with cisplatin versus cisplatin alone in patients with malignant pleural mesothelioma. *J Clin Oncol* 2003; **21**: 2636–2644.
- Carbone M, Kratzke RA, Testa JR. The pathogenesis of mesothelioma. *Semin Oncol* 2002; **29**: 2–17.
- Sekido Y. Genomic abnormalities and signal transduction dysregulation in malignant mesothelioma cells. *Cancer Sci* 2010; **101**: 1–6.
- Bianchi AB, Mitsunaga SI, Cheng JQ, Klein WM, Jhanwar SC, Seizinger B *et al*. High frequency of inactivating mutations in the neurofibromatosis type 2 gene (NF2) in primary malignant mesotheliomas. *Proc Natl Acad Sci USA* 1995; **92**: 10854–10858.
- Sekido Y, Pass HI, Bader S, Mew DJ, Christman MF, Gazdar AF *et al*. Neurofibromatosis type 2 (NF2) gene is somatically mutated in mesothelioma but not in lung cancer. *Cancer Res* 1995; **55**: 1227–1231.
- Dong J, Feldmann G, Huang J, Wu S, Zhang N, Comerford SA *et al*. Elucidation of a universal size-control mechanism in *Drosophila* and mammals. *Cell* 2007; **130**: 1120–1133.
- Saucedo LJ, Edgar BA. Filling out the Hippo pathway. *Nat Rev Mol Cell Biol* 2007; **8**: 613–621.
- Huang J, Wu S, Barrera J, Matthews K, Pan D. The Hippo signaling pathway coordinately regulates cell proliferation and apoptosis by inactivating Yorkie, the *Drosophila* Homolog of YAP. *Cell* 2005; **122**: 421–434.
- Tapon N, Harvey KF, Bell DW, Wahrer DC, Schiripo TA, Haber D *et al*. Salvador promotes both cell cycle exit and apoptosis in *Drosophila* and is mutated in human cancer cell lines. *Cell* 2002; **110**: 467–478.
- Badouel C, Garg A, McNeill H. Herding Hippos: regulating growth in flies and man. *Curr Opin Cell Biol* 2009; **21**: 837–843.
- Zhao B, Ye X, Yu J, Li L, Li W, Li S *et al*. TEAD mediates YAP-dependent gene induction and growth control. *Genes Dev* 2008; **22**: 1962–1971.
- Mizuno T, Murakami H, Fujii M, Ishiguro F, Tanaka I, Kondo Y *et al*. YAP induces malignant mesothelioma cell proliferation by upregulating transcription of cell cycle-promoting genes. *Oncogene* 2012; **31**: 5117–5122.
- Yokoyama T, Osada H, Murakami H, Tatematsu Y, Taniguchi T, Kondo Y *et al*. YAP1 is involved in mesothelioma development and negatively regulated by Merlin through phosphorylation. *Carcinogenesis* 2008; **29**: 2139–2146.
- Murakami H, Mizuno T, Taniguchi T, Fujii M, Ishiguro F, Fukui T *et al*. LATS2 is a tumor suppressor gene of malignant mesothelioma. *Cancer Res* 2011; **71**: 873–883.
- Feng Y, Longmore GD. The LIM protein Ajuba influences interleukin-1-induced NF- $\kappa$ B activation by affecting the assembly and activity of the protein kinase C $\zeta$ /p62/TRAF6 signaling complex. *Mol Cell Biol* 2005; **25**: 4010–4022.
- Locasale JW, Shaw AS, Chakraborty AK. Scaffold proteins confer diverse regulatory properties to protein kinase cascades. *Proc Natl Acad Sci USA* 2007; **104**: 13307–13312.
- Shaw AS, Filbert EL. Scaffold proteins and immune-cell signalling. *Nat Rev Immunol* 2009; **9**: 47–56.
- Levchenko A, Bruck J, Sternberg PW. Scaffold proteins may biphasically affect the levels of mitogen-activated protein kinase signaling and reduce its threshold properties. *Proc Natl Acad Sci USA* 2000; **97**: 5818–5823.
- Burack WR, Shaw AS. Signal transduction: hanging on a scaffold. *Curr Opin Cell Biol* 2000; **12**: 211–216.
- Abe Y, Ohsugi M, Haraguchi K, Fujimoto J, Yamamoto T. LATS2-Ajuba complex regulates gamma-tubulin recruitment to centrosomes and spindle organization during mitosis. *FEBS Lett* 2006; **580**: 782–788.
- Das Thakur M, Feng Y, Jagannathan R, Seppa MJ, Skeath JB, Longmore GD *et al*. Ajuba LIM proteins are negative regulators of the Hippo signaling pathway. *Curr Biol* 2010; **20**: 657–662.
- Zhao B, Wei X, Li W, Udán RS, Yang Q, Kim J *et al*. Inactivation of YAP oncoprotein by the Hippo pathway is involved in cell contact inhibition and tissue growth control. *Genes Dev* 2007; **21**: 2747–2761.
- Oh HJ, Lee KK, Song SJ, Jin MS, Song MS, Lee JH *et al*. Role of the tumor suppressor RASSF1A in Mst1-mediated apoptosis. *Cancer Res* 2006; **66**: 2562–2569.
- Polesello C, Huelsmann S, Brown NH, Tapon N. The *Drosophila* RASSF homolog antagonizes the hippo pathway. *Curr Biol* 2006; **16**: 2459–2465.
- Sasaki H. Mechanisms of trophoblast fate specification in preimplantation mouse development. *Dev Growth Differ* 2010; **52**: 263–273.
- Alvarez-Fernandez M, Halim VA, Krenning L, Aprelia M, Mohammed S, Heck AJ *et al*. Recovery from a DNA-damage-induced G2 arrest requires Cdk-dependent activation of FoxM1. *EMBO Rep* 2010; **11**: 452–458.
- Laoukili J, Stahl M, Medema RH. FoxM1: at the crossroads of ageing and cancer. *Biochim Biophys Acta* 2007; **1775**: 92–102.
- Wang IC, Chen YJ, Hughes D, Petrovic V, Major ML, Park HJ *et al*. Forkhead box M1 regulates the transcriptional network of genes essential for mitotic progression and genes encoding the SCF (Skp2-Cks1) ubiquitin ligase. *Mol Cell Biol* 2005; **25**: 10875–10894.
- Fu Z, Malureanu L, Huang J, Wang W, Li H, van Deursen JM *et al*. Plk1-dependent phosphorylation of FoxM1 regulates a transcriptional programme required for mitotic progression. *Nat Cell Biol* 2008; **10**: 1076–1082.



- 36 Wang IC, Chen YJ, Hughes DE, Ackerson T, Major ML, Kalinichenko VV *et al*. FoxM1 regulates transcription of JNK1 to promote the G1/S transition and tumor cell invasiveness. *J Biol Chem* 2008; **283**: 20770–20778.
- 37 Wang Z, Banerjee S, Kong D, Li Y, Sarkar FH. Down-regulation of Forkhead Box M1 transcription factor leads to the inhibition of invasion and angiogenesis of pancreatic cancer cells. *Cancer Res* 2007; **67**: 8293–8300.
- 38 Hirota T, Kunitoku N, Sasayama T, Marumoto T, Zhang D, Nitta M *et al*. Aurora-A and an interacting activator, the LIM protein Ajuba, are required for mitotic commitment in human cells. *Cell* 2003; **114**: 585–598.
- 39 Ferrand A, Chevrier V, Chauvin JP, Birnbaum D. Ajuba: a new microtubule-associated protein that interacts with BUBR1 and Aurora B at kinetochores in metaphase. *Biol Cell* 2009; **101**: 221–235.
- 40 Benzinger A, Muster N, Koch HB, Yates 3rd JR, Hermeking H. Targeted proteomic analysis of 14-3-3 sigma, a p53 effector commonly silenced in cancer. *Mol Cell Proteomics* 2005; **4**: 785–795.
- 41 Mo JS, Yu FX, Gong R, Brown JH, Guan KL. Regulation of the Hippo-YAP pathway by protease-activated receptors (PARs). *Genes Dev* 2012; **26**: 2138–2143.
- 42 Yu FX, Zhao B, Panupinthu N, Jewell JL, Lian I, Wang LH *et al*. Regulation of the Hippo-YAP pathway by G-protein-coupled receptor signaling. *Cell* 2012; **150**: 780–791.
- 43 Zhao B, Li L, Wang L, Wang CY, Yu J, Guan KL *et al*. Cell detachment activates the Hippo pathway via cytoskeleton reorganization to induce anoikis. *Genes Dev* 2012; **26**: 54–68.
- 44 Boggiano JC, Fehon RG. Growth control by committee: intercellular junctions, cell polarity, and the cytoskeleton regulate Hippo signaling. *Dev Cell* 2012; **22**: 695–702.
- 45 Wada K, Itoga K, Okano T, Yonemura S, Sasaki H. Hippo pathway regulation by cell morphology and stress fibers. *Development* 2011; **138**: 3907–3914.
- 46 Sansores-Garcia L, Bossuyt W, Wada K, Yonemura S, Tao C, Sasaki H *et al*. Modulating F-actin organization induces organ growth by affecting the Hippo pathway. *EMBO J* 2011; **30**: 2325–2335.
- 47 Marie H, Pratt SJ, Betson M, Epple H, Kittler JT, Meek L *et al*. The LIM protein Ajuba is recruited to cadherin-dependent cell junctions through an association with alpha-catenin. *J Biol Chem* 2003; **278**: 1220–1228.
- 48 Fujii M, Toyoda T, Nakanishi H, Yatabe Y, Sato A, Matsudaira Y *et al*. TGF-beta synergizes with defects in the Hippo pathway to stimulate human malignant mesothelioma growth. *J Exp Med* 2012; **209**: 479–494.

Supplementary Information accompanies this paper on the Oncogene website (<http://www.nature.com/onc>)

# Expression of chromobox homolog 7 (CBX7) is associated with poor prognosis in ovarian clear cell adenocarcinoma *via* TRAIL-induced apoptotic pathway regulation

Kanako Shinjo<sup>1,2</sup>, Yoriko Yamashita<sup>1,3</sup>, Eiko Yamamoto<sup>2</sup>, Shinya Akatsuka<sup>1</sup>, Nozomi Uno<sup>1</sup>, Akihiro Kamiya<sup>3</sup>, Kaoru Niimi<sup>2</sup>, Yuka Sakaguchi<sup>2</sup>, Tetsuro Nagasaka<sup>4</sup>, Takashi Takahashi<sup>5</sup>, Kiyosumi Shibata<sup>2</sup>, Hiroaki Kajiyama<sup>2</sup>, Fumitaka Kikkawa<sup>2</sup> and Shinya Toyokuni<sup>1</sup>

<sup>1</sup>Department of Pathology and Biological Responses, Nagoya University Graduate School of Medicine, Showa-ku, Nagoya, Japan

<sup>2</sup>Department of Obstetrics and Gynecology, Nagoya University Graduate School of Medicine, Showa-ku, Nagoya, Japan

<sup>3</sup>Department of Experimental Pathology and Tumor Biology, Nagoya City University Graduate School of Medical Sciences, Mizuho-ku, Nagoya, Japan

<sup>4</sup>Department of Pathophysiological Laboratory Sciences, Nagoya University Graduate School of Medicine, Higashi-ku, Nagoya, Japan

<sup>5</sup>Division of Molecular Carcinogenesis, Center for Neurological Diseases and Cancer, Nagoya University Graduate School of Medicine, Showa-ku, Nagoya, Japan

Ovarian cancer is the most lethal gynecologic malignancy, and clear cell adenocarcinoma of the ovary (OCCA), in particular, has a relatively poor prognosis among the ovarian cancer subtypes because of its high chemoresistance. Chromobox (CBX) 7 is a polycomb repressive complex 1 component that prolongs the lifespan of normal human cells by downregulating the INK4a/ARF expression which promotes cell-cycle progression. However, recent reports studying the relationship between CBX7 expression and patient survival have differed regarding the tumor cell origins, and the precise role of CBX7 in human carcinomas remains obscure. In this study, we analyzed CBX7 expression by immunohistochemistry in 81 OCCA patients and evaluated its association with their clinical outcomes. Both the overall and progression-free survival rates of the CBX7-positive patients were significantly shorter than those of the CBX7-negative patients ( $p < 0.05$ ). CBX7 knockdown experiments using two OCCA cell lines, TOV21G and KOC-7C, revealed that cell viability was significantly reduced compared to the control cells ( $p < 0.001$ ). Expression microarray analysis revealed that apoptosis-related genes, particularly tumor necrosis factor-related apoptosis-inducing ligand (TRAIL), were significantly upregulated in CBX7 knockdown cells ( $p < 0.01$ ). We further confirmed that CBX7 knockdown resulted in TRAIL-induced apoptosis in the OCCA cells. Thus, in this study, we showed for the first time that CBX7 was associated with a decreased OCCA prognosis. We also successfully demonstrated that the TRAIL pathway is a novel target for CBX7 expression modulation in these cells, and therapeutic agents utilizing the TRAIL pathway may be particularly effective for targeted OCCA therapy.

Ovarian cancer is the most lethal gynecologic malignancy. There is no effective screening method, and most women are diagnosed with advanced-stage disease. In Japan, ovarian clear cell adenocarcinoma (OCCA) accounts for ~25% of all

**Key words:** ovarian clear cell adenocarcinoma, chromobox homolog 7 (CBX7), immunohistochemistry, siRNA, expression microarray, TNFSF10 (TRAIL)

Additional Supporting Information may be found in the online version of this article

**Grant sponsor:** Scientific Research from the Japan Society for the Promotion of Science; **Grant number:** 23590394 (to Y.Y.)

**DOI:** 10.1002/ijc.28692

**History:** Received 23 May 2013; Accepted 11 Dec 2013; Online 22 Dec 2013

**Correspondence to:** Yoriko Yamashita, Department of Experimental Pathology and Tumor Biology, Nagoya City University Graduate School of Medical Sciences, 1 Kawasumi, Mizuho-cho, Mizuho-ku, Nagoya, 467-8601, Japan, Tel.: +81-52-853-8146, Fax: +81-52-842-0817, E-mail: k46581a@nucc.cc.nagoya-u.ac.jp

epithelial ovarian cancer (EOC) cases,<sup>1</sup> whereas in North America and Europe, OCCA accounts for only 1–12% of cases.<sup>2</sup> OCCA has been considered to be distinct from high-grade serous adenocarcinoma because of its clinical and biological characteristics. OCCA has been known to be associated with endometriosis,<sup>3,4</sup> and recent studies have suggested that oxidative stress caused by excess iron leads to carcinogenesis in the ovary.<sup>5,6</sup> Advanced stage is associated with poor prognosis in OCCA,<sup>2</sup> and the survival rates in the stages are poorer than those for patients with serous adenocarcinoma,<sup>7</sup> most likely because of OCCA resistance to standard platinum-based chemotherapy.<sup>8</sup> Therefore, it is important to find new therapeutic targets for OCCA.

Chromobox 7 (CBX7) is a member of the polycomb group (PcG) of proteins and is a component of polycomb repressive complex 1 (PRC1). PRC1 can silence the genes that are related to stem cell renewal, differentiation and cancer in conjunction with PRC2.<sup>9</sup> PcG proteins have been reported to be overexpressed and associated with tumorigenesis in a variety of human cancers, mostly by downregulating

### What's new?

Ovarian cancer is the most lethal gynecologic malignancy, with clear cell adenocarcinoma of the ovary (OCCA) having a particularly poor prognosis due to high chemoresistance. Chromobox homolog 7 (CBX7) is a polycomb group transcriptional repressor whose role in human cancer remains controversial. Here, the authors showed for the first time that CBX7 expression is related to worse prognosis in OCCA. Furthermore, knockdown of CBX7 *in vitro* induced apoptosis in OCCA cell lines, possibly via regulation of the TRAIL-pathway. The findings thus indicate CBX7 as a good prognostic marker, and the TRAIL-pathway as a potential target for OCCA diagnosis and therapy.

the tumor suppressor genes.<sup>10</sup> CBX7 has been reported to extend the cellular life span by directly repressing the INK4a/ARF locus.<sup>11</sup> Additionally, CBX7 is an oncogene in several human tumors, including follicular lymphoma, prostate and gastric cancers.<sup>12-14</sup> In follicular lymphoma, CBX7 also cooperates with MYC to produce highly aggressive B-cell lymphoma and can initiate T-cell lymphomagenesis by repressing the INK4a/ARF locus.<sup>13</sup> Recently, it has been reported that CDKN2B-AS (ANRIL), a long noncoding RNA also encoded in the INK4a/ARF locus, acts together with CBX7 to repress INK4a/ARF locus genes, such as CDKN2A (p16; p16INK4a) and ARF (p14 ARF) in prostate cancer cells.<sup>15</sup> Furthermore, a genome-wide association study comparing Japanese women with endometriosis to healthy controls revealed that a single nucleotide polymorphism that showed the strongest association with endometriosis was located in the intron of the ANRIL gene.<sup>16</sup> As OCCA is known to have strong association with endometriosis,<sup>4-6</sup> we speculated that CBX7 and ANRIL may play some important roles in the OCCA tumorigenesis. However, in clear contrast, the loss of CBX7 expression has been reported in association with poorer prognoses and more aggressive behaviors of pancreatic, colorectal, and lung cancers.<sup>17-19</sup> It has been shown that CBX7 represses CDH1 (E-cadherin) expression and CCNE1 (cyclin E1) expression in pancreatic and lung cancers, respectively.<sup>20,21</sup> Therefore, the role of CBX7 in cancer still remains controversial. In this study, we attempted to clarify the role of CBX7 in ovarian cancer, specifically OCCA.

## Material and Methods

### Patients and tissue samples

The ethics committee (Internal Review Board) of the Nagoya University Graduate School of Medicine approved the experiments. The human samples were obtained after each patient provided written informed consent. Formalin-fixed, paraffin-embedded tumor samples from 81 primary OCCA were obtained from the patients who underwent surgical treatment at Nagoya University Hospital from 1986 to 2009 and had clinical follow-up information available. Tumor staging was based on the International Federation of Gynecology and Obstetrics (FIGO) classifications, and reviewed by two expert gynecologists (H.K. and F.K.) for this study. All patients were primarily treated with optimally debulking surgery by skilled

surgeons in gynecologic oncology. Thereafter, 75 (93%) of the 81 patients received adjuvant chemotherapy. Beginning in 1997, most of the patients received platinum- and taxane-based agents or CPT-11 chemotherapy. Before 1997, various cisplatin-based chemotherapies were administered. The following chemotherapy regimens were followed: 7% cyclophosphamide 500 mg/m<sup>2</sup>, adriamycin 50 mg/m<sup>2</sup>, and cisplatin 50 mg/m<sup>2</sup> (CAP), 8% cisplatin and carboplatin (PP), 5% cisplatin, vinblastine, and bleomycin (PVB), 62% paclitaxel 175 mg/m<sup>2</sup>, carboplatin AUC5 (TC), 3% docetaxel 70 mg/m<sup>2</sup>, carboplatin AUC5 (DC), 4% CPT-11 180 mg/m<sup>2</sup>, cisplatin 60 mg/m<sup>2</sup> (CPT-P), 2% other, and 9% unknown. Tumor recurrence or progression was determined by clinical, radiologic, or histologic diagnosis. All histologic diagnoses were specifically reviewed by experts in gynecological pathology (Y.Y. and T.N.) for this study. Endometriosis was defined histologically as the presence of endometrial glands and stromal tissues other than the endometrium or within one-third depth of the uterine myometrium. We also excluded ovarian endometrial cysts lacking epithelium without any atypia for the diagnosis of endometriosis.

### Cell culture and cell lines

The human OCCA cell line TOV-21G and a prostate cancer PC3 line were obtained from the American Type Culture Collection (ATCC, Manassas, VA), and the KOC7C line was a generous gift from Dr. Junzo Kigawa (Tottori University, Tottori, Japan). These cells were cultured in an RPMI-1640 medium (Sigma-Aldrich, St Louis, MO) containing 10% fetal bovine serum at 37°C under a 5% CO<sub>2</sub> atmosphere and were tested and authenticated using the short tandem repeat (STR) method.<sup>22</sup> Human OCCA cell lines JHOC-5, 7, 8, 9 were recently (2009-) obtained from Riken BRC (Tsukuba, Japan) and cultured using Dulbecco's Modified Eagle's Medium/Nutrient F-12 Ham (DMEM:F12) medium (Sigma-Aldrich) with similar conditions. Human endometrial epithelial cells were obtained from normal endometrium of a patient undergoing hysterectomy, and after collagenase treatment, cells were cultured using DMEM:F12 and then infected first with a lentivirus encoding HPV16 E6 and E7 followed by a retrovirus encoding human telomerase similar to previous studies.<sup>23,24</sup> Establishment procedure for the cells (hEEC-N1) was done with written permission, and established cells were confirmed as endometrial epithelial origin by immunohistochemical

analyses for detection of both keratin and vimentin using similar methods as a previous study.<sup>23</sup>

#### Immunohistochemistry and RNA fluorescence *in situ* hybridization (RNA-FISH)

For immunohistochemistry (IHC), we used anti-CBX7 (ab21873, Abcam, Cambridge, MA) as the primary antibody. DNA probes for RNA-FISH were prepared by PCR amplifying cDNA templates to obtain ~500 bp sized-PCR products using primers 5'-GAATTTGGGAATGAGGAGCA-3' and 5'-AAGCTGCAAAGGCCCTCAATA-3' for ANRIL and 5'-TCAG AAGGATTCCTATGTGG-3' and 5'-TCTCCTTAATGTAC GCACG-3' for human  $\beta$ -actin, and then labeled with SpectrumOrange using Vysis Nick Translation Kit (Abbott, Abbott Park, IL). For fluorescence IHC and RNA fluorescence *in situ* hybridization (RNA-FISH), cells were grown on a chamber slide, and fixed with 4% paraformaldehyde. For RNA-FISH, after permeabilization using cytoskeletal buffer, slides were hybridized with the labeled probes. For fluorescence IHC, cells were visualized with Alexa Fluor labeled secondary antibody (Life Technologies, Carlsbad, CA). Finally, cells were counterstained with DAPI and then visualized with a fluorescence microscope.

For formalin-fixed, paraffin-embedded ovarian tumor sections, we used polymer-based methods with the EnVision System (DAKO, Glostrup, Denmark). CBX7 staining was interpreted by three independent pathologists (Y.Y., T.N., and S.T.) blinded to clinical data. Because interobserver variability was rather large in samples with 10–50% nuclear staining, we defined the samples that contained nuclear staining >10% of cancer cells as positive, and the others negative.

#### Small interference RNA (siRNA) transfection

To knockdown CBX7, we used two individual siRNAs: One was an endoribonuclease-prepared siRNA (esiRNA) against CBX7 (EHU035461, Sigma-Aldrich), and the other was designed using the sense sequence 5'-GCATTTGCCATC TGCCTT-3'; we named these siRNAs siCBX7-1 and siCBX7-2, respectively. We used MISSION siRNA Universal Negative Control (SIC-001, Sigma-Aldrich) as the negative control. KOC7C and TOV21G were transfected with the siRNAs using the Lipofectamine RNAiMAX reagent (Invitrogen, Carlsbad, CA) at a final concentration of 10 nM, according to the manufacturer's instructions. Analyses were performed 48 hr after transfection.

#### Quantitative reverse transcriptase-PCR

Total RNA was extracted from the cell lines using the RNeasy Plus Mini Kit (QIAGEN, Hilden, Germany) according to the manufacturer's instructions. Then, cDNA was synthesized from 500 ng total RNA using the Superscript III First-Strand Synthesis System for RT-PCR (Life Technologies), and quantitative PCR was performed as previously described.<sup>25</sup> The sequences of primers were as follows: CBX7, forward 5'-GGATGGCCCCCAAAGTACAG-3' and reverse

5'-TATACCCCGATGCTCGGTCTC-3'; ANRIL, forward 5'-CAACATCCACCACTGGATCTTAACA-3' and reverse 5'-AGCTTCGTATCCCCAATGAGATAACA-3'; CDKN2A, forward 5'-CATAGATGCCGCGGAAGGT-3' and reverse 5'-CCCGA GGTTCCTCAGAGCCT-3'; TNFSF10A, forward 5'-C CTCA GAGAGTAGCAGCTCACA-3' and reverse 5'-GCCCCA GAG CCTTTTCATTC-3'; for  $\beta$ -actin, forward 5'-CGGGAC CT GACTGACTA-3' and reverse 5'-GAAGGAAGGCTGGA AG AGT-3'; and TNFSF10, forward 5'-CCTCAGAGAGTAG CA GCTCACA-3' and reverse 5'-GCCAGAGCCTTTTCAT TC-3'. The data from the PCR reaction were normalized against the  $\beta$ -actin expression using the comparative Ct method. The transcripts were quantified in duplicates.

#### Western blot analysis

Whole-cell or tissue lysates were prepared similarly as previously described<sup>26</sup> from cell lines and primary tumor tissues from four OCCA patients. Twenty-microgram proteins were separated using sodium dodecyl sulfate polyacrylamide gel electrophoresis and blotted on Immobilon P filters (Millipore, Billerica, MA). The following antibodies were used: anti-Cbx7 (1:1,000) (ab21873, Abcam), anti- $\beta$ -actin (1:2,000) (A5316, Sigma-Aldrich) and anti-PARP (1:1,000) (#9542, Cell Signaling Technology, Beverly, MA). ImmunoStar LD (Wako, Osaka, Japan) was used for chemiluminescence detection.

#### Cell viability assay

A total of 4,000 cells were transfected with siRNAs in 96-well plates and incubated under 5% CO<sub>2</sub> at 37°C. After 24, 48, 72, and 96 hr, cell viability was assayed by MTS [3-(4,5-dimethylthiazol-2-yl)-5-(3-carboxymethoxyphenyl)-2-(4-sulfo-phenyl)-2H-tetrazolium] assay using the CellTiter 96 Aqueous One Solution Cell Proliferation Assay kit (Promega, Madison, WI), according to the manufacturer's instructions.

#### Migration and invasion assay

The assays were performed using 6.5 mm Transwell plates with 8.0  $\mu$ m pore polycarbonate membrane inserts (Corning Coaster, Rochester, NY). For the invasion assay, the upper surfaces of the filters were coated with 50  $\mu$ l of matrigel (Becton and Dickenson, Franklin Lakes, NJ). Next, 1  $\times$  10<sup>5</sup> cells were seeded in the upper chamber in the culture medium without FBS, and the lower chamber contained 10% FBS. The cells were incubated for 24 hr at 37°C in 5% CO<sub>2</sub>. After removing the noninvaded or nonmigrated cells, the remaining cells were stained with Giemsa.

#### Cell cycle analysis

A total of 5  $\times$  10<sup>5</sup> cells were washed with PBS, fixed with 70% ethanol at -20°C for at least 30 min, washed again with PBS, and incubated with 0.1 mg/ml RNase A solution (QIAGEN) at 37°C for 20 min. The cells were centrifuged, washed again with PBS, and then incubated with 50  $\mu$ g/ml of propidium iodide (Sigma-Aldrich) on ice for 20 min. The cell cycle profiles were determined using a FACS Calibur